Article

Modeling the Metal Center of Cys Zinc Proteins

Andrew S. Lipton, and Paul D. Ellis

J. Am. Chem. Soc., **2007**, 129 (29), 9192-9200• DOI: 10.1021/ja071430t • Publication Date (Web): 27 June 2007

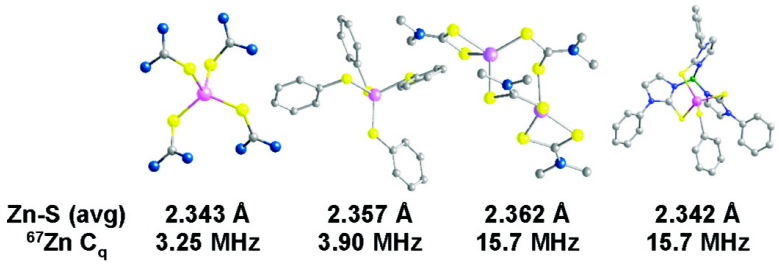

More About This Article

Additional resources and features associated with this article are available within the HTML version:

- Supporting Information
- Links to the 5 articles that cite this article, as of the time of this article download
- Access to high resolution figures
- Links to articles and content related to this article
- Copyright permission to reproduce figures and/or text from this article

View the Full Text HTML

J|A|C|S
ARTICLES
Published on Web 06/27/2007

Modeling the Metal Center of Cys_4 Zinc Proteins

Andrew S. Lipton and Paul D. Ellis*

Contribution from Macromolecular Structure & Dynamics Directorate, Fundamental Sciences Division, Pacific Northwest National Laboratory, Richland, Washington 99352

Received February 28, 2007; E-mail: paul.ellis@pnl.gov

Abstract: We present here a ^{67}Zn solid-state NMR investigation of several model complexes of zinc coordinated by four sulfurs. The lineshapes were obtained at a variety of magnetic fields from 11.7 T (500 MHz for ^1H) to 21.15 T (900 MHz for ^1H) and at ambient temperature down to 10 K. The quadrupole coupling constants, C_q's, ranged from 3.25 to 16.7 MHz throughout the series, while the average bond distances only spanned 2.34−2.36 Å. Reasonable agreement with experiment was achieved in the molecular orbital calculations using DFT methods and the local density approximation to predict electric field gradients.

Introduction

Cysteine coordination to zinc was long thought to be primarily a structural motif. Most notable among these are zinc finger proteins that have varying stoichiometries of cysteine (C) and histidine (H) ligands (C_4, C_3H, or C_2H_2). One of the exciting recent developments in zinc bioinorganic chemistry has been the recognition that certain ZnC_4 sites are involved in catalysis of alkyl group transfer. This represents a new class of biological zinc sites. The first alkyl-transfer protein to be characterized was the DNA methylation repair protein Ada.[1] Since the discovery of thiolate alkylation in Ada, several other zinc-containing alkyl-transfer proteins have been identified. These include methionine synthase (MetE),[2,3] farnesyl transferase,[4] methylcobamide:CoM methyltransferase,[5] betaine homocysteine methyl transferase,[6] and epoxide carboxylase.[7] A common feature of the mechanisms of action of these enzymes appears to be the reaction of a zinc-bound thiolate ligand.

The zinc site is typically thiolate rich, and in some cases the zinc is coordinated exclusively to thiolates. These sites while appearing to have structural motif are nevertheless reactive, promoting the alkylation of a cysteine that is, at least transiently, bound to the zinc. What distinguishes the thiolate environments in a structural site from a catalytic site remains an unanswered question in zinc chemistry. The Ada protein carries out multiple reactions,[8] where the C-terminal domain repairs base alkylation and the N-terminal domain repairs alkylated phosphotriesters by alkyl transfer to Cys38.[9] This cysteine is one of four that ligate an essential zinc.[9,10] The Ada alkylation reaction is stoichiometric and irreversible rather than catalytic. However, alkylation of Cys38 induces a conformational change in Ada, causing a dramatic increase in its DNA affinity, which in turn promotes transcription of methylation repair genes, including Ada.[11]

The observation that one of the thiolate ligands in Ada is methylated may seem surprising, since one might expect that coordination of a cysteine thiolate to a zinc cation would significantly decrease its nucleophilicity. However, examples of zinc-bound thiolates reacting with alkyl donors have been known in the inorganic literature for many years.[12,13] Recently, Wilker and Lippard have investigated the kinetics of phosphate demethylation by zinc thiolate complexes.[14−16] For thiolate methylation by $(CH_3O)_3PO$, they find that reactivity increases in the order $Zn(SR)_2N_2 \ll Zn(SR)_3N^- < Zn(SR)_4^{2-}$ where "SR" is an aromatic thiolate and "N" is an imidazole.[14] All of the zinc complexes are more reactive than free thiol, but all are less reactive than free thiolate. This led to the suggestion that the active nucleophile is free thiolate, produced through the reaction below, where "L, L′, and L″" may be a mixture of thiolate and histidine ligands and "*n*" is the overall charge.

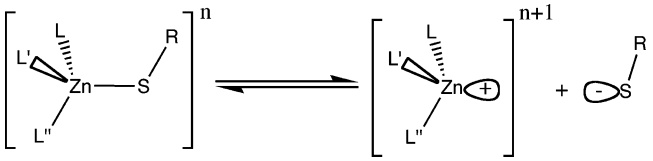

The above equilibrium will shift, depending on the number of anionic ligands in "L, L′, and L″", thus accounting for the

(1) Myers, L. C.; Terranova, M. P.; Nash, H. M.; Markus, M. A.; Verdine, G. L. *Biochemistry* **1992**, *31*, 4541−4547.
(2) Gonzalez, J. C.; Peariso, K.; Penner-Hahn, J. E.; Matthews, R. G. *Biochemistry* **1996**, *35*, 12228−12234.
(3) Goulding, C. W.; Matthews, R. G. *Biochemistry* **1997**, *36*, 15749−15757.
(4) Huang, C.-C.; Casey, P. J.; Fierke, C. A. *J. Biol. Chem.* **1997**, *272*, 20−23.
(5) LeClerc, G. M.; Grahame, D. A. *J. Biol. Chem.* **1996**, *271*, 18725−18731.
(6) Millian, N. S.; Garrow, T. A. *Arch. Biochem. Biophys.* **1998**, *356*, 93−98.
(7) Allen, J. R.; Ensign, S. A. *J. Biol. Chem.* **1997**, *272*, 32121−32128.
(8) Myers, L. C.; Terranova, M. P.; Ferentz, A. E.; Wagner, G.; Verdine, G. L. *Science* **1993**, *261* (5125), 1164−1167.
(9) Myers, L. C.; Cushing, T. D.; Wagner, G.; Verdine, G. L. *Chem. Biol* **1994**, *1*, 91−97.
(10) Myers, L. C.; Verdine, G. L.; Wagner, G. *Biochemistry* **1993**, *32*, 14089−14094.
(11) Myers, L. C.; Jackow, F.; Verdine, G. L. *J. Biol. Chem.* **1995**, *270*, 6664−6670.
(12) Lindoy, L. F. *Coord. Chem. Rev.* **1969**, *4*, 41−71.
(13) Lindoy, L. F.; Busch, D. H. *Inorg. Chem.* **1974**, *13*, 2494−2498.
(14) Wilker, J. J.; Lippard, S. J. *J. Am. Chem. Soc.* **1995**, *117*, 8682−8683.
(15) Wilker, J. J.; Lippard, S. J. *Inorg. Chem.* **1997**, *36*, 969−978.
(16) Wilker, J. J.; Wetterhahn, K. E.; Lippard, S. J. *Inorg. Chem.* **1997**, *36*, 2079−2083.

10.1021/ja071430t CCC: $37.00

decrease in activity as the number of histidine ligands increases. Support for this mechanism comes from a detailed kinetic and equilibrium study that determined the equilibrium constant K_d for the above reaction to be 1.0 ($\pm$0.9) $\times$ 10^{-2} M.[15] This remarkably large dissociation constant means that for 5 mM $Zn(SPh)_4^{2-}$, nearly 75% of the Zn is present as the $[Zn(SPh)_3(solvent)]^-$ complex. The rate of methylation of $Zn(SPh)_4^{2-}$ by $(CH_3O)_3$-PO is 70% as fast as that of free thiolate. This means that free thiolate, produced as above, can account for *all* of the methylation activity of $Zn(SPh)_4^{2-}$. This has led to the suggestion that free thiolate may also be the active nucleophile in Ada, and perhaps in the other alkyl-transfer proteins.[15,16] Although this mechanism has received some endorsement,[17,18] there are some difficulties with this proposal.

A disassociated cysteine in water would be present as an unreactive thiol at neutral pH. The role of zinc is likely to help modulate the electrostatics (hydrogen bonding to the various thiolates will also contribute to a moderation of the electrostatics) of one or more of the bound thiolates, thereby selecting or activating one of the four cysteines for the reaction. If the reactive species were a free thiolate, then there would be no role for zinc in directly activating it. Further, there are model compounds in which thiolate can also be methylated, such as neutral Zn−thiolate complexes with either two[19] or three[20] nitrogen ligands. Although these molecules, particularly a series of tris-pyrazolylborate complexes, are not expected to have significant thiolate dissociation, they are nevertheless efficiently methylated, leading to suggestions that it may be the zinc bound thiolate rather than free thiolate that is the nucleophile.[20] In addition, some of the alkyl transfer enzymes (e.g., MetE[2] and farnesyl transferase,[21,22]) appear to have monoanionic sites, rather than the more reactive dianionic sites suggested by the Wilker/Lippard model. For farnesyl transferase, replacement of a neutral histidine ligand with an anionic glutamate *decreases* the rate of cysteine alkylation by a factor of nearly 10^4, in contrast with the acceleration that might be expected for the anionic substitution.[23] Finally, the basis of the Wilker/Lippard model is the fact that the above equilibrium provides the proper amount of thiolate to account for the observed reactivity. The equilibrium constant $K_d = 1.0\ (\pm 0.9) \times 10^{-2}$ M is thus crucial to this mechanism. Unfortunately, it was not possible to obtain a precise determination of K_d from NMR spectroscopy.[15] If the true K_d is at the lower limit of the estimated range (e.g., 1.0×10^{-3} M), then free thiolate would account for only a small fraction of the observed methylation in this system.

Another attempt to model these systems has been made by the Parkin group who have created a synthetic analogue of the Ada DNA repair protein, namely $[Tm^{Ph}]$ZnSPh, in which SPh^- mimics the active cysteine.[24,25] A functional equivalence with the protein is provided by the observation that the complex is rapidly alkylated, albeit by methyl iodide, yet the relatively short Zn−SPh bond (2.258 Å) implies that the reaction does not proceed via a dissociative mechanism. Neither this nor the concerns mentioned above invalidate the Wilker/Lippard model. They do demonstrate, however, that the role of zinc in thiolate activation remains an open question, both for the model complexes and especially for the proteins.

It is for that reason we have decided to apply ^{67}Zn NMR methods as a means to further characterize the nature of the coordination environment around the Zn^{2+} in zinc thiolates. To understand what differentiates a catalytic C_4 zinc site from a structural one, a comparison to known systems is needed. The first step to this is to correlate structure with magnetic resonance parameters (in this case the electric field gradient). Following this is comparing experiment with molecular theory to find the level of theory (and basis set) required to adequately predict the observed quadrupolar parameters. To this end we have examined the Zn^{2+} sites in a variety of model compounds via solid-state ^{67}Zn NMR spectroscopy with the aim of shedding some light on the differences these compounds may or may not have relative to one another. The model compounds we have investigated are $Zn[SC(NH_2)_2]_4(NO_3)_2$ (**1**),[26] $Zn[SPh]_4(Me_4N)_2$ (**2**),[27,28] $Zn[SPhMe]_4(Me_4N)_2$ (**3**),[29] $Zn[S_2CN(CH_3)_2]_2$ (**4**),[30] and $[Tm^{Ph}]$ZnSPh (**5**).[24] These compounds have the additional property that the average Zn−S bond distance is 2.35 $\pm$ 0.01 Å. As we will subsequently show, even with such an average isotropy in the bond distance, the ^{67}Zn NMR parameters are responsive to the individual specifics of each environment and not just the average. Finally we show which factors appear to give rise to this distribution utilizing various levels of theory.

Experimental Section

^{67}Zn[SC(NH$_2$)$_2$]$_4$(NO$_3$)$_2$ (1).[31] This compound was prepared in the same fashion as Sham and Wu[32] by dissolving $^{67}Zn(NO_3)_2$ in methanol and adding 4 equiv of thiourea.

Zn[SPh]$_4$(Me$_4$N)$_2$ (2). There were two preparations of this sample, the first was a gift from Professor Daniel Reger following the procedure of Dance et al.,[27] and the second source was a gift from Professor Gerard Parkin following the same procedure with a 5% doping of the cobalt analogue.[33]

^{67}Zn[SPhMe]$_4$(Me$_4$N)$_2$ (3). This compound was prepared following the methods of Dance et al.[27] for $Zn[SPh]_4$ utilizing 4-methyl benzenethiol and $^{67}Zn(NO_3)_2$ as starting materials.

Zn[S$_2$CN(CH$_3$)$_2$]$_2$ (4). This sample was a gift from Professor Daniel Reger.

[Tm^{Ph}]ZnSPh (5). This sample was a gift from Professor Gerard Parkin prepared with a 2% doping of the cobalt analogue.

Solid-State ^{67}Zn NMR. All zinc chemical shifts are referenced with respect to 1 M $Zn(NO_3)_{2(aq)}$ (measured at ambient temperature). The ^{67}Zn powder spectra acquired at ambient temperature utilized a Varian Unity^{plus} spectrometer with a wide-bore Oxford Instruments magnet

(17) Hightower, K. E.; Fierke, C. A. *Curr. Opin. Chem. Biol.* **1999**, *3*, 176−181.
(18) Matthews, R. G.; Goulding, C. W. *Curr. Opin. Chem. Biol.* **1997**, *1*, 332−339.
(19) Grapperhaus, C. A.; Tuntulani, T.; Reibenspies, J. H.; Darensbourg, M. Y. *Inorg. Chem.* **1998**, *37*, 4052−4058.
(20) Brand, U.; Rombach, M.; Vahrenkamp, H. *Chem. Commun.* **1998**, 2717−2718.
(21) Strickland, C. L.; Windwor, W. T.; Syto, R.; Wang, L.; Bond, R.; Wu, Z.; Schwartz, J.; Beese, L. S.; Le, H. V.; Weber, P. C. *Biochemistry* **1998**, *37*, 16601−16611.
(22) Long, S. B.; Casey, P. J.; Beese, L. S. *Biochemistry* **1998**, *37*, 9612−9618.
(23) Fu, H.-W.; Beese, L. S.; Casey, P. J. *Biochemistry* **1998**, *37*, 4465−4472.
(24) Bridgewater, B. M.; Fillebeen, T.; Friesner, R. A.; Parkin, G. *J. Chem. Soc., Dalton Trans.* **2000**, *24*, 4494−4496.
(25) Parkin, G. *Chem. Rev.* **2004**, *104*, 699−767.
(26) Vega, R.; Lopez-Castro, A.; Marquez, R. *Acta Crystallogr.* **1978**, *B34*, 2297−2299.
(27) Dance, I. G.; Choy, A.; Scudder, M. L. *J. Am. Chem. Soc.* **1984**, *106*, 6285−6295.
(28) Ueyama, N.; Sugawara, T.; Sasaki, K.; Nakamura, A.; Yamashita, S.; Wakatsuki, Y.; Yamazaki, H.; Yasuoka, N. *Inorg. Chem.* **1988**, *27*, 741−747.
(29) Prepared in the same fashion as Dance et. al. using 4-methyl benzenethiol instead of benzenethiol.
(30) Klug, H. P. *Acta Crystallogr.* **1966**, *21*, 536−546.
(31) The complexes that utilized isotopic enrichment were labeled with ^{67}Zn at 88% (Cambridge Isotopes).
(32) Sham, S.; Wu, G. *Can. J. Chem.* **1999**, *77*, 1782−1787.
(33) Dance, I. G. *J. Am. Chem. Soc.* **1979**, *101*, 6264−6273.

operating at 11.7 T (500 MHz for ^{1}H and 31.297 MHz for ^{67}Zn), a Varian Unity^{Inova} spectrometer with a medium-bore (63 mm) Oxford Instruments magnet operating at 18.8 T (800 MHz for ^{1}H and 50.048 MHz for ^{67}Zn), or a Varian Unity^{Inova} spectrometer with a medium-bore (63 mm) Oxford Instruments magnet operating at 21 T (900 MHz for ^{1}H and 56.316 MHz for ^{67}Zn). The respective NMR probes used were a 5 mm Doty Scientific (DSI; Columbia, SC) wide line probe at 11.7 T and home built 5 mm wide-line probes at the higher fields. To obtain cryogenic temperatures (10 K) in the 11.7 and 18.8 T magnets an Oxford Instruments continuous flow cryostat was utilized. The cryostat is top-loaded into the bore of the magnet, and a home built NMR probe is then inserted into the sample space of the cryostat.[34,35]

The pulse sequences used were quadrupole echo (QE),[36−38] quadrupole Carr−Purcell−Meiboom−Gill (QCPMG),[39,40] and cross polarization (CP)[41] combined with either quadrupole echo or QCPMG. Double frequency sweep (DFS)[42,43] was also used to generate magnetization followed by either QE or QCPMG. The spectra were analyzed using the SIMPSON program.[44] Simulations of the NMR spectra were performed on a Beowulf cluster at PNNL (composed of 24-Racksaver Dual Pentium IV 2.4 GHz Xeon nodes and 8-Racksaver Dual Pentium III 1.26 GHz nodes) running the Rocks clustering software and utilizing a gigabit Ethernet connection. The errors in the extracted parameters were estimated from the response of the residual sum of squares (RSS). To minimize the errors optimizations were conducted utilizing data from multiple fields simultaneously for each iteration of the parameters. The estimated errors in the extracted parameters are as follows, except where indicated: $C_q \pm 0.02$ MHz, $\eta_q \pm 0.02$, $\delta_{iso} \pm 2$ ppm, $\Delta\sigma \pm 0.5$ ppm, $\eta_\sigma \pm 0.02$, and $\alpha\beta\gamma \pm 5°$. We define the shielding anisotropy as $\Delta\sigma = \delta_{33} - 1/2\ (\delta_{11} + \delta_{22})$, where the elements of the shielding tensor are ordered as $|\delta_{33} - \delta_{iso}| \geq |\delta_{11} - \delta_{iso}| \geq |\delta_{22} - \delta_{iso}|$. For experiments that were acquired with a single transmitter frequency the simulations were performed with finite pulse widths. Those experiments that required combining stepped frequencies were simulated with ideal pulses.

Ab Initio Calculations. The calculations of the electric field gradient (EFG) tensors were performed using NorthWestChem (NWChem) developed at Pacific Northwest National Laboratory.[45,46] Where available the X-ray geometry was utilized for a field gradient calculation. The density matrix used for the calculation of the field gradient was computed after the SCF portion of the calculation had converged to an rms level of 10^{-8} or better. The calculations were carried out on the following systems; an 8 CPU Silicon Graphics Origin 2000 computer, the Beowulf cluster mentioned above (using only the P4 nodes), a 128 CPU Silicon Graphics Altix computer, or the 11.8 TFlop Hewlett-Packard system (980 dual Intel 1.5 GHz Itanium-2 processors) present in the Environmental Molecular Sciences Laboratory (EMSL) running a version of Linux based on Red Hat Linux Advanced Server with a QSNet^{II}/Elan-4 interconnect from Quadrics.

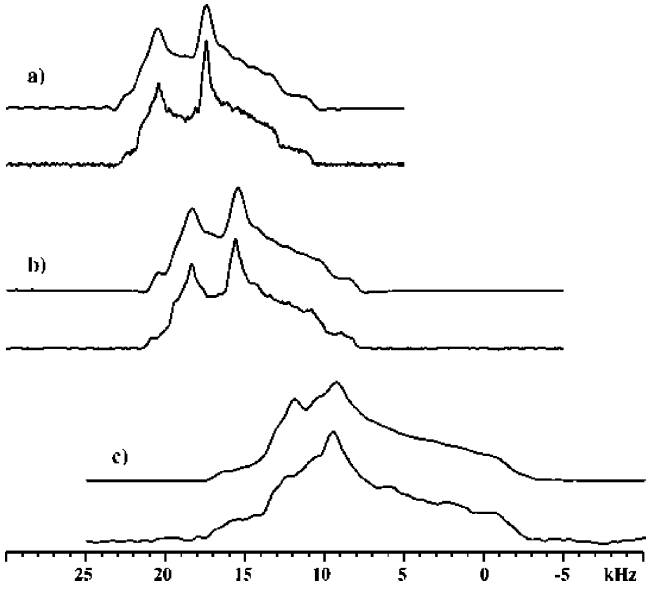

Figure 1. Experimental and simulated ^{67}Zn QE NMR data for **1** where (a) was collected at 21.15 T (RT) with a selective $\pi/2$ pulse of 9.5 μs and a pulse delay of 1 s for 32768 transients, and has 50 Hz of exponential linebroadening (LB); (b) was collected at 18.8 T (RT) with a selective $\pi/2$ pulse of 7.3 μs and a recycle delay of 1 s for 21300 transients and 100 Hz of LB; (c) was collected at 11.7 T (RT) with a selective $\pi/2$ pulse of 3.2 μs and a pulse delay of 1 s for 65536 transients with 500 Hz of LB. Simulations are above their respective experiments, and the optimized parameters used are listed in Table 1.

The basis sets utilized for the EFG calculations were typically of at least a triple-ζ level. The basis sets used were the Schafer, Horn, and Ahlrichs valence triple-ζ (AVTZ)[47] as well as an updated version from Schafer, Huber, and Ahlrichs (ATZV),[48] each with added polarization functions. The ATZV basis set did not contain hydrogen; thus, the AVTZ basis set was used for those atoms. These basis sets with polarization functions are available for download from the EMSL using the basis set order form[49] or as part of the Extensible Computational Chemistry Environment (ECCE) software package.[50] The final collection of basis sets used were the nonrelativistic correlation consistent triple- or quadruple-ζ functions of Peterson and co-workers (cc-pVTZ-NR or cc-pVQZ-NR).[51,52]

Results and Discussion

The data shown in Figure 1 is of $^{67}Zn[SC(NH_2)_2]_4(NO_3)_2$ acquired at room temperature at (a) 21.15, (b) 18.8, and (c) 11.7 T along with their respective simulations. The simulations were fit using all three experimental data sets simultaneously to give a quadrupole coupling constant, C_q, of 3.25 MHz and asymmetry parameter, η_q, of 0.89. The full list of the extracted parameters for all of the thiolate complexes is presented in Table 1. Where chemical shielding anisotropy (CSA) could be reliably extracted,

(34) Lipton, A. S.; Sears, J. A.; Ellis, P. D. *J. Magn. Reson.* **2001**, *151*, 48−59.
(35) Lipton, A. S.; Heck, R. W.; Sears, J. A.; Ellis, P. D. *J. Magn. Reson.* **2004**, *168*, 66−74.
(36) Solomon, I. *Phys. Rev.* **1958**, *110*, 61−65.
(37) Weisman, I. D.; Bennett, L. H. *Phys. Rev.* **1969**, *181*, 1344−1350.
(38) Kunwar, A. C.; Turner, G. L.; Oldfield, E. *J. Magn. Reson.* **1986**, *69*, 124−127.
(39) Larsen, F. H.; Jakobsen, H. J.; Ellis, P. D.; Nielsen, N. C. *J. Phys. Chem. A* **1997**, *101*, 8597−8606.
(40) Larsen, F. H.; Lipton, A. S.; Jakobsen, H. J.; Nielsen, N. C.; Ellis, P. D. *J. Am. Chem. Soc.* **1999**, *121*, 3783−3784.
(41) Pines, A.; Gibby, M. G.; Waugh, J. S. *J. Chem. Phys.* **1972**, *56*, 1776.
(42) Iuga, D.; Schäfer, H.; Verhagen, R.; Kentgens, A. P. M. *J. Magn. Reson* **2000**, *147*, 192−209.
(43) Schäfer, H.; Iuga, D.; Verhagen, R.; Kentgens, A. P. M. *J. Chem. Phys.* **2001**, *114*, 3073−3091.
(44) Bak, M.; Rasmussen, J. T.; Nielsen, N. C. *J. Magn. Reson.* **2000**, *147*, 296−330.
(45) Aprà, E.; et al. *NWChem, A Computational Chemistry Package for Parallel Computers*, version 4.6; Pacific Northwest National Laboratory: Richland, Washington 99352−0999, U.S.A., 2004.
(46) Kendall, R. A.; Aprà, E.; Bernholdt, D. E.; Bylaska, E. J.; Dupuis, M.; Fann, G. I.; Harrison, R. J.; Ju, J.; Nichols, J. A.; Nieplocha, J.; Straatsma, T. P.; Windus, T. L.; Wong, A. T. *Comput. Phys. Commun.* **2000**, *128*, 260−283.
(47) Schafer, A.; Horn, H.; Ahlrichs, R. *J. Chem. Phys.* **1992**, *97*, 2571−2577.
(48) Schafer, A.; Huber, C.; Ahlrichs, R. *J. Chem. Phys.* **1994**, *100*, 5829−5835.
(49) http://www.emsl.pnl.gov/forms/basisform.html.
(50) Basis sets were obtained from the *Extensible Computational Chemistry Environment Basis Set Database*, version 02/25/04, as developed and distributed by the Molecular Science Computing Facility, Environmental and Molecular Sciences Laboratory which is part of the Pacific Northwest Laboratory, P.O. Box 999, Richland, Washington 99352, U.S.A., and is funded by the U.S. Department of Energy. The Pacific Northwest Laboratory is a multiprogram laboratory operated by Battelle Memorial Institute for the U.S. Department of Energy under Contract DE-AC06-76RLO 1830. Contact Karen Schuchardt for further information.
(51) Peterson, K. A.; Puzzarini, C. *Theor. Chem. Acc.* **2005**, *114*, 283−296.
(52) Balabanov, N. B.; Peterson, K. A. *J. Chem. Phys.* **2005**, *123*, 064107.

Table 1. Experimental ^{67}Zn NMR Tensor Parameters for Zinc Thiolates

complex	C_q	η_q	δ_{iso}	$\Delta\sigma$	η_σ	α	β	γ
1	3.25(3.15)[a]	0.89(1.00)	337.1(350)	−56.8	0.86	7.3	15.4	−1.2
2 (RT)	3.90	0.65	333.0	76.0	0.17	136.9	106.8	1.9
2 (10 K)	4.57	0.69	346.8	−34.8	0.06	−12.2	−13.4	5.4
3 (site 1)	3.95	0.15	339.0	−22.7	.115	192.0	129.9	43.2
3 (site 2)	6.80	0.11	340.0	−31.0	.190	223.5	52.0	150.2
4 (10 K)	15.7 ± 0.5	0.94 ± 0.05	70 ± 20					
5 (site 1, 10 K)	15.7 ± 0.5	0.10 ± 0.05	400 ± 20					
5 (site 2, 10 K)	16.7 ± 0.5	0.33 ± 0.05	495 ± 20					
5 (site 1, RT)	15.5 ± 0.5	0.14 ± 0.05	364 ± 5					
5 (site 2, RT)	15.8 ± 0.5	0.03 ± 0.05	318.5 ± 5					

[a] Numbers in parenthesis are from Sham and Wu, ref 32.

Table 2. Electric Field Gradient Calculations on **1**

complex	basis	method	C_q	η_q
$Zn[SC(NH_2)_2]_4$ (+2)	AVTZ	RHF	1.420	0.155
$Zn[SC(NH_2)_2]_4$ (+2)	ATZV	RHF	1.318	0.129
$Zn[SC(NH_2)_2]_4$ (+2)	cc-pVTZ-NR[a]	RHF	1.830	0.487
$Zn[SC(NH_2)_2]_4$ (+2)	cc-pVTZ-NR[b]	RHF	2.299	0.356
$Zn[SC(NH_2)_2]_4$ (+2)	cc-pVQZ-NR[a]	RHF	2.059	0.262
$Zn[SC(NH_2)_2]_4$ (+2)	AVTZ	LDA	3.920	0.796
$Zn[SC(NH_2)_2]_4$ (+2)	ATZV	LDA	−3.229	0.951
$Zn[SC(NH_2)_2]_4$ (+2)	AVTZ	B3LYP	2.131	0.993
$Zn[SC(NH_2)_2]_4$ (+2)	ATZV	B3LYP	1.984	0.735
$Zn[SC(NH_2)_2]_4(NO_3)_2$	AVTZ	RHF	7.537	0.796
$Zn[SC(NH_2)_2]_4(NO_3)_2$	ATZV	RHF	7.860	0.760
$Zn[SC(NH_2)_2]_4(NO_3)_2$	AVTZ	LDA	8.643	0.998
$Zn[SC(NH_2)_2]_4(NO_3)_2$	ATZV	LDA	8.391	0.950
$Zn[SC(NH_2)_2]_4(NO_3)_2$	AVTZ	B3LYP	9.194	0.919
$Zn[SC(NH_2)_2]_4(NO_3)_2$	ATZV	B3LYP	9.114	0.861
$\{Zn[SC(NH_2)_2]_4\}_2(NO_3)_{14}$ (−10)	AVTZ	RHF	1.640	0.902
$\{Zn[SC(NH_2)_2]_4\}_2(NO_3)_{14}$ (−10)	cc-pVTZ-NR[a]	RHF	6.310	0.130
$\{Zn[SC(NH_2)_2]_4\}_2(NO_3)_{14}$ (−10)	ATZV	LDA	−4.881	0.265

[a] This basis set for Zn only; all other atoms were AVTZ with polarization. [b] This basis set for Zn and S only; all other atoms were AVTZ with polarization.

those numbers are reported; otherwise no attempt to estimate CSA has been made.

Also listed in Table 1 is the previous result from Sham and Wu for **1** where the lineshape was obtained under magic angle spinning conditions.[32] The fit from this data did not include any effects of CSA (as the contribution to the lineshape was removed by the sample spinning), which we found necessary in our earlier analysis of our natural abundance data.[53] The previous lineshape parameters we reported were an estimation of the CSA contributions due to the low S/N and the fact that data from a single magnetic field was available at the time. The sensitivity afforded by the isotopic label meant that these data could now be acquired at all fields without operating at cryogenic temperatures. For other samples where labeling was not performed, room temperature acquisitions were attempted, and if more sensitivity was required, the low-temperature experiments were carried out.

In our continuing efforts to understand the structural factors contributing to the field gradient tensor we have performed several ab initio molecular orbital calculations. These calculations varied in several ways; various levels of basis set used, method (DFT vs RHF), and inclusion of potential hydrogen-bonding partners from the counterions. These results are summarized in Table 2 for the thiourea (tu) complex (**1**).

Starting with the X-ray geometry of the dication species, the trend for restricted Hartree−Fock (RHF) seems to underestimate the field gradient by more than a factor of 2 as well as grossly missing the asymmetry parameter. With the use of the correlation consistent basis sets (cc-V*n*Z-NR; n = T or Q) on the zinc both the EFG and η_q improve, however, not in a clear trend that leads one to believe that we are adequately describing the system. Surprisingly, DFT with the exchange-correlation functional defined as the local spin density approximation (LSDA or LDA) utilizing Slater's local spin density exchange,[54] the Vosko, Wilk, and Nusair (VWN) V local spin density correlation functional,[55] and the same basis sets as RHF seems to greatly improve both the C_q and η_q to the point that they are converging on the experimental numbers. However, Becke's three-parameter hybrid functional[56] using the Lee, Yang, and Parr (LYP) correlation functional,[57] B3LYP, does not seem to do as well. To test the impact of the counterion and potential hydrogen-bonding partners, calculations were performed on the neutral system as well as increasing to two molecules with 14 anions. For the neutral species, including two anions, the field gradients are overestimated; however, the predicted asymmetry parameter is reasonable for all the DFT calculations. Running the calculations on the dimer with RHF, the C_q brackets the experimental value going from too small by a factor of 2 to double the value with the correlation consistent basis set. The η_q value starts close to experiment for the Ahlrichs triple-ζ, but is again unreasonable when using correlation consistent basis. Using DFT/LDA brings the predicted C_q back down; however, the asymmetry parameter is missed again.

The solid-state NMR experiments on $Zn[SC_6H_5]_4[N(CH_3)_4]_2$ were acquired both at ambient and cryogenic[34,35] (10 K) temperatures, which gave different results. The sample used for the low-temperature experiments was doped with 5% of the Co analogue to shorten the ^{1}H T_1 which in turn enabled a faster recycle time.[58] The room-temperature results from the 21.15 and 18.8 T systems are shown in Figure 2a and 2b with their respective simulations. The average C_q extracted here is 3.9 MHz with an η_q value of 0.65 where again the optimization was performed on the two data sets simultaneously. The low-temperature data from the 18.8 and 11.7 T systems are depicted in Figure 2c and 2d respectively. The extracted C_q increases to almost 5 MHz, while the η_q value increases slightly to 0.69 (both data sets were optimized simultaneously). These changes

(53) Lipton, A. S.; Buchko, G. W.; Sears, J. A.; Kennedy, M. A.; Ellis, P. D. *J. Am. Chem. Soc.* **2001**, *123*, 992−993.
(54) Slater, J. C. *The Self-Consistent Field for Molecules and Solids*; McGraw-Hill: New York, 1974; Vol. 4.
(55) Vosko, S. H.; Wilk, L.; Nusair, M. *Can. J. Phys.* **1980**, *58*, 1200−1211.
(56) Becke, A. D. *J. Chem. Phys.* **1993**, *98*, 5648.
(57) Lee, C.; Yang, W.; Parr, R. G. *Phys. Rev. B* **1988**, *37*, 785.
(58) Lipton, A. S.; Wright, T. A.; Bowman, M. K.; Reger, D. L.; Ellis, P. D. *J. Am. Chem. Soc.* **2002**, *124*, 5850−5860.

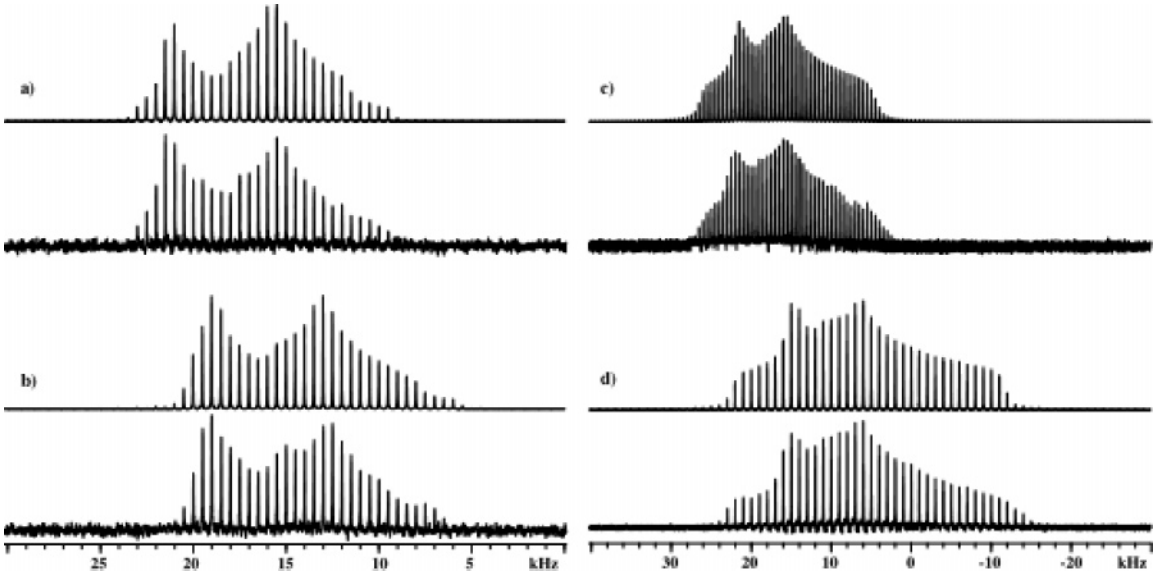

Figure 2. Experimental and simulated ^{67}Zn spin echo NMR data for **2** where (a) is CP/QCPMG collected at 21.15 T (RT) with a ^{1}H RF field of 41.7 kHz, 20 μs selective ^{67}Zn π pulses and a recycle time of 5 s for 16384 transients; (b) is DFS/QCPMG collected at 18.8 T (RT) with a 22 kHz RF fields, DFS sweeps from 50 kHz to 1 MHz offsets in 750 μs and a recycle time of 1 s for 65536 transients; (c) is a skyline projection of four transmitter offsets of 10 kHz steps of CP/QCPMG collected at 18.8 T (10 K) with a ^{1}H RF field of 51 kHz, 20 μs selective π pulses, a recycle time of 15 s, and 512 transients for each offset; (d) is a skyline projection of four transmitter offsets of 10 kHz steps of CP/QCPMG collected at 11.7 T (10 K) with a ^{1}H RF field of 50 kHz, 10 μs selective π pulses, a recycle time of 10 s, and 2048 transients for each offset.

are most likely due to either a phase transition or slight changes in local geometry or unit cell parameters as the temperature is reduced.

From the X-ray structure of **2** there are pairs of ZnS bonds that are similar (two short at 2.344 Å and two longer at 2.367 and 2.378 Å) to the $Zntu_4$ structure. This is a different pattern from the $ZnSPh_4$ of Coucouvanis[59] where there were three longer bonds (2.362, 2.363, and 2.357 Å) and one shorter (2.329 Å). The difference between the two is simply the counterion $NMe_4]^{+}$ here versus $PPh_4]^{+}$. Clearly steric interactions play a role by influencing the geometry, but is that the only effect of the counterion? The long bonds, Zn−S1 and Zn−S4, form a tighter angle between their phenyl rings than the other pair (101° vs 112°). This forces the counterion to sit more than 1 Å further from the zinc than the other side (7.056 Å instead of 5.888 Å).

Once again to determine the extent of any contributions from the counterions a series of ab initio molecular orbital calculations were performed with and without the $NMe_4]^{+}$ present. The results of these calculations are compared with experimental numbers in Table 3. Utilizing the X-ray geometry we find that RHF methods overestimate C_q in both cases (with and without the $NMe_4]^{+}$'s), however the DFT/LDA method falls right in between the room-temperature and low-temperature results with just the dianion (no counterions included). The same DFT/LDA calculations on the neutral system overestimate C_q by almost a factor of 2. Curiously, the inverse trend is true for the prediction of the asymmetry parameter; the inclusion of the counterions brings the value of η_q down from the overestimate given when it is not included.

By expanding the unit cell out using symmetry, one finds that there is a ring of four cations sitting around the zinc (each Zn−N distance ≤ 6Å) from the neighboring molecules. The six cations take the positions of an octahedral geometry where each of the "equatorial" cations resides directly opposite the plane of a phenyl ring from one of the "axial" cations. This is shown in Figure 3 where the hydrogen atoms have been omitted for clarity. Adding these extra charges to the calculations improves both DFT methods (LDA and hybrid) to very good agreement with experiment; however, only the LDA comes close to predicting the asymmetry parameter.

Table 3. Electric Field Gradient Calculations on **2**

complex	basis	method	C_q	η_q
$Zn(SPh)_4$ (−2)	AVTZ	RHF	6.475	0.675
$Zn(SPh)_4$ (−2)	ATZV	RHF	6.219	0.721
$Zn(SPh)_4$ (−2)	AVTZ	LDA	−4.505	0.830
$Zn(SPh)_4$ (−2)	ATZV	LDA	−4.507	0.781
$Zn(SPh)_4$ (−2)	AVTZ	B3LYP	4.849	0.915
$Zn(SPh)_4$ (−2)	ATZV	B3LYP	4.718	0.973
$Zn(SPh)_4[N(CH_3)_4]_2$	AVTZ	RHF	9.108	0.409
$Zn(SPh)_4[N(CH_3)_4]_2$	ATZV	RHF	8.723	0.417
$Zn(SPh)_4[N(CH_3)_4]_2$	AVTZ	LDA	7.751	0.360
$Zn(SPh)_4[N(CH_3)_4]_2$	ATZV	LDA	7.516	0.381
$Zn(SPh)_4[N(CH_3)_4]_2$	AVTZ	B3LYP	8.153	0.432
$Zn(SPh)_4[N(CH_3)_4]_2$	ATZV	B3LYP	7.908	0.445
$Zn(SPh)_4[N(CH_3)_4]_6$ (+4)	AVTZ	RHF	6.065	0.744
$Zn(SPh)_4[N(CH_3)_4]_6$ (+4)	ATZV	RHF	5.665	0.796
$Zn(SPh)_4[N(CH_3)_4]_6$ (+4)	AVTZ	LDA	−3.848	0.638
$Zn(SPh)_4[N(CH_3)_4]_6$ (+4)	ATZV	LDA	−3.701	0.652
$Zn(SPh)_4[N(CH_3)_4]_6$ (+4)	AVTZ	B3LYP	−4.261	0.939
$Zn(SPh)_4[N(CH_3)_4]_6$ (+4)	ATZV	B3LYP	−4.126	0.934

The need to include the extra cations is understandable as the aromatic rings are themselves polarizable as are the sulfurs. The π-electrons from the aromatic ring are sensitive to the charges on either side of the phenyl group, and they in turn polarize the attached sulfur. The zinc is sensitive to this and it is reflected in the field gradient.

The next compound in this series is the tetrakis(4-toluenethiolato-S-)zinc (**3**) which currently does not have a known crystal structure. From the zinc NMR spectra shown in Figure 4 we see the appearance of two forms with a ratio of close to 1:1. These forms are assumed to be different structures within the

(59) Swenson, D.; Baenziger, N. C.; Coucouvanis, D. *J. Am. Chem. Soc.* **1978**, *100*, 1932−1934.

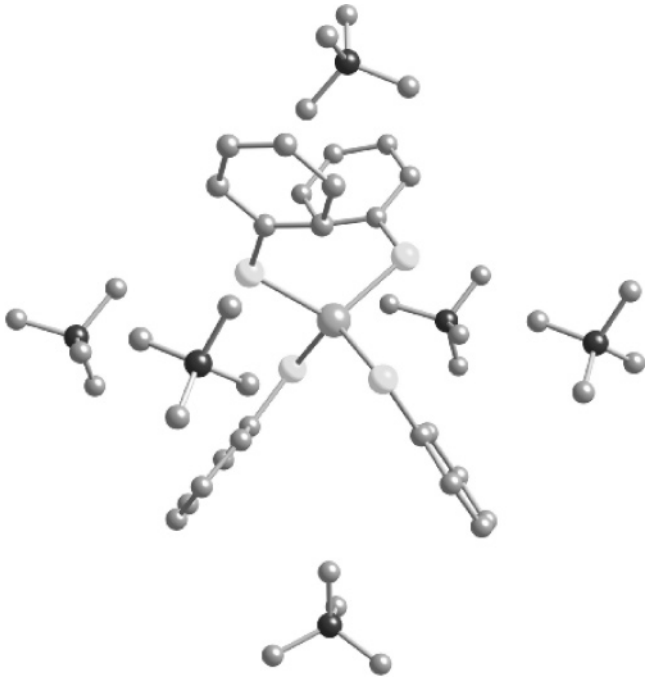

Figure 3. Structure of tetrakisthiophenol zinc with six of the closest tetramethylammonium cations occupying the vertices of an octahedral geometry around the zinc. Hydrogen atoms have been omitted for clarity.

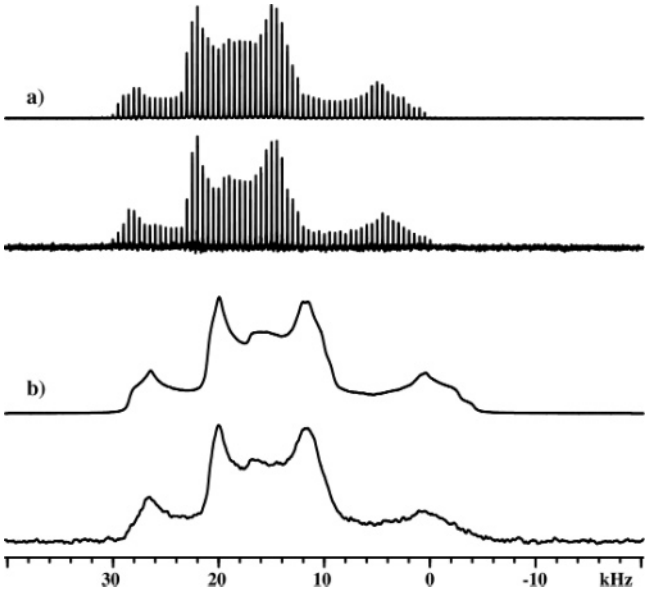

Figure 4. Experimental and simulated ^{67}Zn spin echo NMR data for **3** where (a) is a CP/QCPMG collected at 21.15 T (RT) with a ^{1}H field of 41.7 kHz, 10 μs selective ^{67}Zn π pulses, and a recycle time of 30 s for 1024 transients and (b) is CP/QCPMG collected at 18.8 T (RT) with a ^{1}H field of 50 kHz, 4 μs selective ^{67}Zn π pulses, and a recycle time of 10 s for 4480 transients.

same unit cell as there is no evidence for separate species in the ^{1}H NMR when the sample is dissolved in DMSO-d_6. Further evidence comes from the lineshape simulations and the extraction of the shielding anisotropy parameters. Curiously the two lineshapes when fit independently return similar values for the shielding anisotropy, the asymmetry parameter, and Euler angles relating the two PAS frames. The values reported in Table 1 reflect an independent optimization of these parameters (forcing them to be identical between the sites also gives a reasonable fit, within our errors). One site seems to have a C_q similar to that of the thiophenol; however, this species shows a highly symmetric environment with η_q less than 0.2. The other site shows a larger field gradient with C_q estimated near 7 MHz. By using the X-ray structure of **2** and adding methyl groups in the para position of each phenyl, we recalculated the field gradient using both LDA and B3LYP methods for each triple-ζ basis set. These results are tabulated in Table 4 along with the calculations with a series on the neutral species and with six cations in the same octahedral-like positions as in Figure 3. The simple dianionic system (no counterions) predicts a C_q around 4.6 MHz for the LDA and approximately 4.8 MHz for the hybrid functional. For each case the η_q value is not even close to the experimental value; however, even including the same counterions that were in the thiophenol case, the η_q values only came down to what was predicted for **2**. This new model with six cations now brackets the experimental value of C_q, with LDA predicting 3.6−3.7 MHz and B3LYP at 4.1−4.3 MHz for each triple-ζ basis set.

Table 4. Electric Field Gradient Calculations on **3**

complex	basis	method	C_q	η_q
$Zn(SC_6H_5CH_3)_4$ (−2)	AVTZ	LDA	−4.578	0.813
$Zn(SC_6H_5CH_3)_4$ (−2)	ATZV	LDA	−4.573	0.770
$Zn(SC_6H_5CH_3)_4$ (−2)	AVTZ	B3LYP	4.872	0.936
$Zn(SC_6H_5CH_3)_4$ (−2)	ATZV	B3LYP	4.749	0.990
$Zn(SC_6H_5CH_3)_4[N(CH_3)_4]_2$	AVTZ	LDA	−4.542	0.822
$Zn(SC_6H_5CH_3)_4[N(CH_3)_4]_2$	ATZV	LDA	−4.924	0.811
$Zn(SC_6H_5CH_3)_4[N(CH_3)_4]_2$	AVTZ	B3LYP	4.891	0.953
$Zn(SC_6H_5CH_3)_4[N(CH_3)_4]_2$	ATZV	B3LYP	4.729	0.966
$Zn(SC_6H_5CH_3)_4[N(CH_3)_4]_6$ (+4)	AVTZ	LDA	−3.559	0.642
$Zn(SC_6H_5CH_3)_4[N(CH_3)_4]_6$ (+4)	ATZV	LDA	−3.690	0.664
$Zn(SC_6H_5CH_3)_4[N(CH_3)_4]_6$ (+4)	AVTZ	B3LYP	−4.275	0.942
$Zn(SC_6H_5CH_3)_4[N(CH_3)_4]_6$ (+4)	ATZV	B3LYP	−4.134	0.943

Optimizing the geometry of **3** without cations using the DFT/LDA with a double-ζ basis set yielded pairs of Zn−S bonds on 2.405 and 2.397 Å. The LDA functional has been shown to give a more representative geometry for Zn−S bonds in zinc thiolates.[60] The pairs of bonds were on ligands where the aromatic rings were "stacked". Performing a field gradient calculation on this optimized geometry with the AVTZ basis set and the LDA method predicts a C_q of 7.3 MHz, which is surprisingly close to the second species observed experimentally. The value of η_q is predicted to be 0.34; however, there were no counterions included in the calculation. Repeating the geometry optimization on the neutral system, with cations between the "stacked" rings, the average Zn−S bond length was reduced by 0.013 Å, and the predicted AVTZ/LDA C_q was ∼3.1 MHz with an η_q of 0.36. Finally, the optimized geometry of **3** with six counterions predicts a C_q of 4.7 MHz with an η_q of 0.29 and an average bond distance decreased 0.003 Å from that of the neutral system.

The dithiocarbamate, **4**, presented a greater challenge due to poor signal-to-noise (S/N) and the potential presence of overlapping (yet similar) lineshapes. From the data shown in Figure 5 one can see the absence of features to distinguish the lineshapes at either field. Therefore the errors reported for **4** are significantly higher than for the previous complexes. Interestingly while the two sites are related by symmetry in the crystallography,[30] molecular theory predicts different C_q's for each site. This shows the sensitivity to the field gradients based on

(60) Dudev, T.; Lim, C. *J. Phys. Chem. B* **2001**, *105*, 10709−10714.

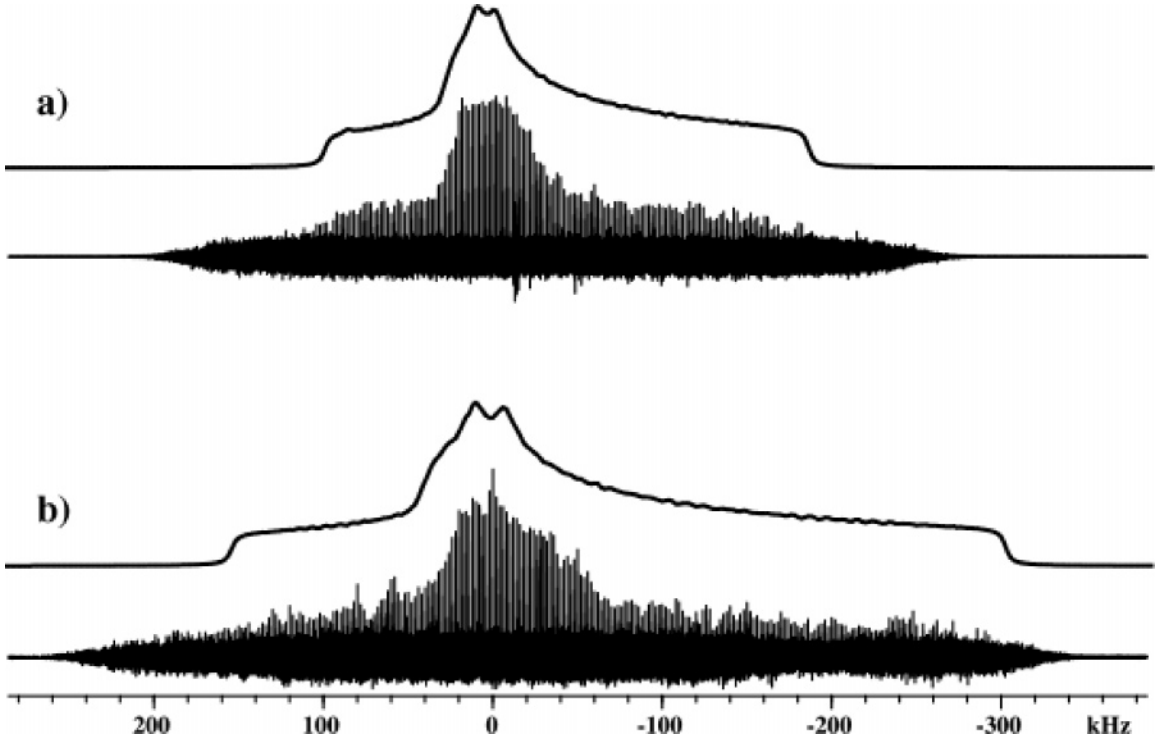

Figure 5. Experimental and simulated ^{67}Zn QCPMG NMR data for **4** where (a) is a skyline projection of 40 transmitter offsets of 10 kHz steps of CP/QCPMG collected at 18.8 T (10 K) with a ^{1}H RF field of 32 kHz, 20 μs selective π pulses, a recycle time of 60 s, and 256 transients for each offset and (b) is a skyline projection of 50 transmitter offsets of 10 kHz steps of CP/QCPMG collected at 11.7 T (10 K) with a ^{1}H field of 50 kHz, 10 μs selective π pulses, a recycle time of 60 s, and 256 transients for each offset. Simulations for each are ideal pulse, quadrupole-only lineshapes as indicated in Table 1.

Table 5. Electric Field Gradient Calculations on **4**

complex	basis	method	C_q	η_q
$\{Zn[S_2CN(Me_2)]_2\}_2$ site 1	AVTZ	RHF	21.913	0.895
$\{Zn[S_2CN(Me_2)]_2\}_2$ site 2	AVTZ	RHF	21.736	0.915
$\{Zn[S_2CN(Me_2)]_2\}_2$ site 1	AVTZ	LDA	11.497	0.790
$\{Zn[S_2CN(Me_2)]_2\}_2$ site 2	AVTZ	LDA	11.306	0.797
$\{Zn[S_2CN(Me_2)]_2\}_2$ site 1	AVTZ	B3LYP	15.041	0.837
$\{Zn[S_2CN(Me_2)]_2\}_2$ site 2	AVTZ	B3LYP	14.829	0.856
$\{Zn[S_2CN(Me_2)]_2\}_2$ site 1	ATZV	RHF	21.090	0.919
$\{Zn[S_2CN(Me_2)]_2\}_2$ site 2	ATZV	RHF	20.895	0.940
$\{Zn[S_2CN(Me_2)]_2\}_2$ site 1	ATZV	LDA	12.180	0.764
$\{Zn[S_2CN(Me_2)]_2\}_2$ site 2	ATZV	LDA	12.006	0.775
$\{Zn[S_2CN(Me_2)]_2\}_2$ site 1	ATZV	B3LYP	15.339	0.830
$\{Zn[S_2CN(Me_2)]_2\}_2$ site 2	ATZV	B3LYP	15.134	0.851

the proton positions (which were not determined crystallographically). The protons were added in idealized positions on the methyl carbons with a C−H distance of 1.170 Å. The values for C_q are tabulated in Table 5. While theory does not predict the C_q's for **4** as well as for the previous compounds, the increase in magnitude is matched by theory. This increase is most likely due to the fact that the sulfurs from these ligands do not each donate a negative charge, but only a fraction of one due to the bidentate nature of the ligand. Each ligand donates a single negative charge that is delocalized between the pair of sulfurs coordinating to the metal. Perhaps as a consequence of this, the hybrid functional, B3LYP, seems to do better at predicting the field gradient than the local density approximation.

In fitting this data it was apparent that a quadrupole-only line shape could not adequately fit the experimental data (see Figure 5); however, a contribution from shielding anisotropy, while plausible physically, could not be reliably extracted from the data. Again, the lack of features in the center of the lineshapes causes this uncertainty and could be due to the second site having slightly different quadrupole and/or shielding parameters. It is not beyond reason that at the temperature these experiments were performed the symmetry between the sites has been broken.

Complex **5** has a tridentate ligand with a single negative charge delocalized among each of the three sulfurs that coordinate to the zinc. This species also displays a larger field gradient than most of the previous complexes. The zinc spectra for **5** are depicted in Figure 6 along with the respective simulations, the extracted NMR parameters are summarized in Table 1, and the predicted EFG parameters from molecular theory are listed in Table 6. One thing should be apparent at this point, and that is the NMR data reflects the presence of more than one species while the crystallography (and therefore molecular theory) only shows a single structure. The data acquired at 10 K reflects two species with C_q's of 15.7 and 16.7 MHz and η_q values of 0.10 and 0.33, respectively. The ratio between the two sites is approximately 1:2 with the more asymmetric site reflecting the dominant form. This is consistent with theory as this site is fairly well predicted using DFT/LDA methods and either triple-ζ basis set. The room-temperature data (collected at 21.15 T or 900 MHz for ^{1}H) also reflect two species; however, the η_q values are more similar, with each showing a high degree of symmetry. The ratio between the sites is more like 3:1 though, with the species with the isotropic chemical shift of 364 ppm being the dominant form.

The presence of these other species as well as the disorder exhibited in the experimental data can probably be attributed to the method in which the sample was prepared. In doping the sample with its cobalt analogue, the material was not allowed to recrystallize. Instead the sample was dried from CH_2Cl_2,

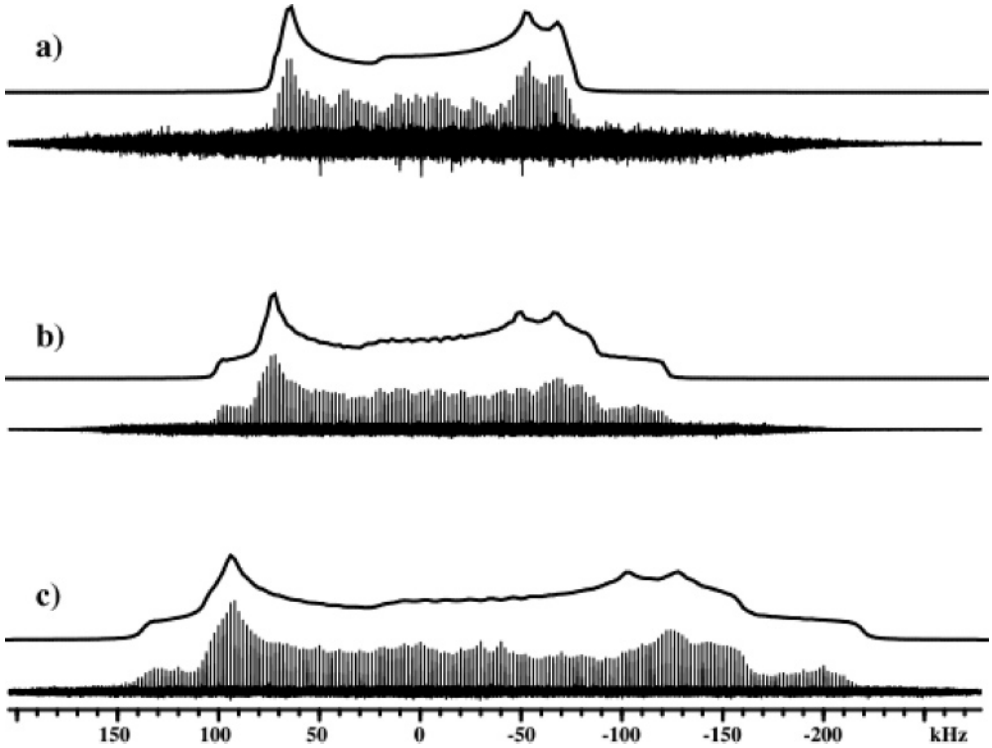

Figure 6. Experimental and simulated ^{67}Zn QCPMG NMR data for **5** where (a) is a skyline projection of three transmitter offsets of 50 kHz steps of DFS/QCPMG collected at 21.15 T (RT) with a 62.5 kHz RF fields, DFS sweeps from 100 kHz to 1.5 MHz offsets in 500 μs, and a recycle time of 2 s for 65536 transients at each offset; (b) is a skyline projection of 23 transmitter offsets of 10 kHz steps of CP/QCPMG collected at 18.8 T (10 K) with a ^{1}H RF field of 32 kHz, 20 μs selective π pulses, a recycle time of 30 s, and 128 transients for each offset; and (c) is a skyline projection of 36 transmitter offsets of 10 kHz steps of CP/QCPMG collected at 11.7 T (10 K) with a ^{1}H field of 31 kHz, 10 μs selective π pulses, a recycle time of 10 s, and 2048 transients for each offset.

Table 6. Electric Field Gradient Calculations on **5**

complex	basis	method	C_q	η_q
[Tm^{Ph}]ZnSPh	AVTZ	RHF	24.258	0.173
[Tm^{Ph}]ZnSPh	AVTZ	LDA	16.484	0.378
[Tm^{Ph}]ZnSPh	AVTZ	B3LYP	18.954	0.289
[Tm^{Ph}]ZnSPh	ATZV	RHF	22.792	0.202
[Tm^{Ph}]ZnSPh	ATZV	LDA	16.265	0.370
[Tm^{Ph}]ZnSPh	ATZV	B3LYP	18.540	0.292

which could have resulted in the presence of rotational isomers (about the Zn−SPh bond) relative to the single conformation found in the X-ray structure.[24] This implies that at room temperature the barrier to rotation about that bond is low enough to facilitate such averaging. To estimate what this barrier to rotation might be we have performed a series of calculations to map the energetics of this process. The phenyl group was rotated in 10° increments, and then the total energy and C_q were calculated. The results are shown in Figure 7 where the maximum energy barrier only occurs in one area ($\theta \approx 150°$) and goes up to ~85 kcal/mol. There are also two other minimal barriers at only ~4.2 kcal/mol that appear at $\theta = 50$ and $-70°$, where θ is the deviation from the reported structure. The value of C_q spans 15.8 to 16.6 over the range, and hits the minimum only when approaching the large barrier from one side. A similar set of calculations was performed, varying the Zn−SPh bond distance to explore the effect on the field gradient of the metal. In the range of 2.25−2.4 Å the value of C_q seems to vary linearly going from 16.9 to 10.4 MHz as the bond length increases. This is consistent with the observed values around 16 MHz as the distance from the X-ray structure is 2.258 Å. While this sensitivity to a single bond complicates the analysis

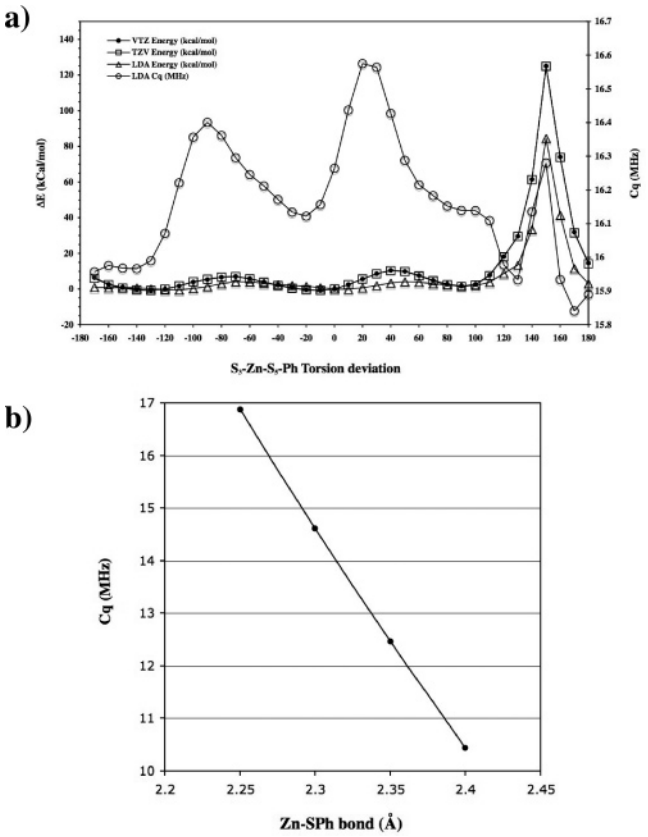

Figure 7. Molecular orbital calculations on **5**, showing (a) the change in energy and the dependence of C_q on the rotation of the SPh ligand where the angle given is the deviation from the X-ray geometry. (b) Predicted changes in C_q over a range of Zn−SPh bond distances.

of this particular compound, it is also a good indicator of what might be expected in a system where a cysteine is poised to dissociate as has been proposed for the mechanism of Ada.

Conclusions

We have demonstrated that field gradients can be predicted fairly well for zinc with four sulfurs in the first coordination sphere. The method of choice seems to be the DFT/LDA method, although the hybrid functional, B3LYP, will also serve to predict qualitative trends. All of the methods seem to miss the mark when dealing with systems with delocalized charges, though. Further analysis is also needed to test the prediction of the field gradients in the presence of mixed coordination (sulfur with nitrogen and oxygen donor atoms, such as N_2S_2 or NS_2O). There is also a sensitivity of the zinc EFG to nonbonding interactions, especially in the case of the thiophenol where there was an interaction between the aromatic rings and the $NMe_4]^+$ cations. The results here show that a model constructed simply on the basis of average bond distances could not explain the diversity of the observed quadrupole coupling constants. Rather, it is clear that several other factors, e.g., polarizability of the S-ligand, the presence or absence of hydrogen bonding to the S, can have dramatic consequences. This was seen in both the dithiocarbamate and mercapto phenylimidazolyl hydroborato ligands where the sulfurs were not bridging, but did not carry a full negative charge. The implication of this is that a cysteine sulfur coordinating a zinc, which has a strong hydrogen bond to it, would have its charge ameliorated. Finally, if there is a significant change in the distribution of bond distances in the series of Ada, Ada·DNA, and Ada·DNA′ (where DNA′ denotes methylated DNA) it should be clear that the ^{67}Zn NMR spectroscopy would be sensitive enough to observe and to interpret the effects of the change in structure about the Zn site.

Acknowledgment. This work was supported by a grant from the National Institutes of Health (Federal Grant EB002050). The NMR experiments were carried out in the Environmental Molecular Sciences Laboratory (a national scientific user facility sponsored by the Department of Energy Office of Biological and Environmental Research) located at Pacific Northwest National Laboratory and operated for DOE by Battelle. The authors would like to gratefully acknowledge Prof. Daniel Reger of the University of S. Carolina for providing the sample of zinc dimethyldithiocarbamate as well as one of the zinc tetrakisthiophenol samples. The authors would also like to gratefully acknowledge Prof. Gerard Parkin of the Columbia University for providing a sample of the tris(2-mercapto-1-phenylimidazolyl)hydroborato complex, $Tm^{Ph}ZnSPh$, as well as the Co^{2+} doped sample of zinc tetrakisthiophenol. NWChem Version 4.7, as developed and distributed by Pacific Northwest National Laboratory, P. O. Box 999, Richland, Washington 99352 USA, and funded by the U.S. Department of Energy, was used to obtain some of these results.

Supporting Information Available: Complete ref 45. This material is available free of charge via the Internet at http://pubs.acs.org.

JA071430T